$\sum w_j Z_j/A_j = \sum n_j Z_j / \sum n_j A_j$. However, $\langle I\rangle$ as defined this way is an underestimate, because in a compound electrons are more tightly bound than in the free elements, and $\langle\delta\rangle$ as calculated this way has little relevance, because it is the electron density which matters. If possible, one uses the tables given in Refs. 13 and 12, which include effective excitation energies and interpolation coefficients for calculating the density effect correction for the chemical elements and nearly 200 mixtures and compounds. If a compound or mixture is not found, then one uses the recipe for δ given in Ref. 10 (or Ref. 8), and calculates $\langle I\rangle$ according to the discussion in Ref. 11. (Note the "13%" rule!)

Ionization losses by electrons and positrons [12] are not discussed here. Above the critical energy, which is a few tens of MeV in most materials, bremsstrahlung is the dominant source of energy loss. This important case is discussed below. The contributions of various electron energy-loss processes in lead are shown in Fig. 11.4.

10.3. Restricted energy loss rates for relativistic ionizing particles

Fluctuations in energy loss are due mainly to the production of a few high-energy knock-on electrons. Practical detectors often measure the energy *deposited*, not the energy *lost*. When energy is carried off by energetic knock-on electrons, it is more appropriate to consider the mean energy loss excluding energy transfers greater than some cutoff $T_{\rm cut}$. The restricted energy loss rate is

$$-\left.\frac{dE}{dx}\right|_{T<T_{\rm cut}} = Kz^2\frac{Z}{A}\frac{1}{\beta^2}\left[\frac{1}{2}\ln\frac{2m_ec^2\beta^2\gamma^2T_{\rm upper}}{I^2} - \frac{\beta^2}{2}\left(1+\frac{T_{\rm upper}}{T_{\rm max}}\right)-\frac{\delta}{2}\right] \qquad (10.5)$$

where $T_{\rm upper} = {\rm MIN}(T_{\rm cut}, T_{\rm max})$. This form agrees with the equation given in previous editions of this *Review* [17] for $T_{\rm cut} \ll T_{\rm max}$ but smoothly joins the normal Bethe-Bloch function (Eq. (10.1)) for $T_{\rm cut} > T_{\rm max}$.

10.4. Energetic knock-on electrons (δ rays)

The distribution of secondary electrons with kinetic energies $T \gg I$ is given by [1]

$$\frac{d^2N}{dTdx} = \frac{1}{2}Kz^2\frac{Z}{A}\frac{1}{\beta^2}\frac{F(T)}{T^2} \qquad (10.6)$$

for $I \ll T \le T_{\rm max}$, where $T_{\rm max}$ is given by Eq. (10.2). The factor F is spin-dependent, but is about unity for $T \ll T_{\rm max}$. For spin-0 particles $F(T) = (1-\beta^2T/T_{\rm max})$; forms for spins 1/2 and 1 are also given by Rossi [1]. When Eq. (10.6) is integrated from $T_{\rm cut}$ to $T_{\rm max}$,one obtains the difference between Eq. (10.1) and Eq. (10.5). For incident electrons, the indistinguishability of projectile and target means that the range of T extends only to half the kinetic energy of the incident particle. Additional formulae are given in Ref. 18. Equation (10.6) is inaccurate for T close to I: for $2I \lesssim T \lesssim 10I$, the $1/T^2$ dependence above becomes approximately $T^{-\eta}$, with $3 \lesssim \eta \lesssim 5$ [19].

10.5. Ionization yields

Physicists frequently relate total energy loss to the number of ion pairs produced near the particle's track. This relation becomes complicated for relativistic particles due to the wandering of energetic knock-on electrons whose ranges exceed the dimensions of the fiducial volume. For a qualitative appraisal of the nonlocality of energy deposition in various media by such modestly energetic knock-on electrons, see Ref. 20. The mean local energy dissipation per local ion pair produced, W, while essentially constant for relativistic particles, increases at slow particle speeds [21]. For gases, W can be surprisingly sensitive to trace amounts of various contaminants [21]. Furthermore, ionization yields in practical cases may be greatly influenced by such factors as subsequent recombination [22].

10.6. Multiple scattering through small angles

A charged particle traversing a medium is deflected by many small-angle scatters. Most of this deflection is due to Coulomb scattering from nuclei, and hence the effect is called multiple Coulomb scattering. (However, for hadronic projectiles, the strong interactions also contribute to multiple scattering.) The Coulomb scattering distribution is well represented by the theory of Molière [23]. It is roughly Gaussian for small deflection angles, but at larger angles (greater than a few θ_0, defined below) it behaves like Rutherford scattering, having larger tails than does a Gaussian distribution.

If we define

$$\theta_0 = \theta_{\rm plane}^{\rm rms} = \frac{1}{\sqrt{2}}\theta_{\rm space}^{\rm rms} . \qquad (10.7)$$

then it is sufficient for many applications to use a Gaussian approximation for the central 98% of the projected angular distribution, with a width given by [24,25]

$$\theta_0 = \frac{13.6\ {\rm MeV}}{\beta cp}\, z\, \sqrt{x/X_0}\Big[1+0.038\ln(x/X_0)\Big] . \qquad (10.8)$$

Here p, βc, and z are the momentum, velocity, and charge number of the incident particle, and x/X_0 is the thickness of the scattering medium in radiation lengths (defined below). This value of θ_0 is from a fit to Molière distribution [23] for singly charged particles with $\beta = 1$ for all Z, and is accurate to 11% or better for $10^{-3} < x/X_0 < 100$.

Eq. (10.8) describes scattering from a single material, while the usual problem involves the multiple scattering of a particle traversing many different layers and mixtures. Since it is from a fit to a Molière distribution, it is incorrect to add the individual θ_0 contributions in quadrature; the result is systematically too small. It is much more accurate to apply Eq. (10.8) once, after finding x and X_0 for the combined scatterer.

Lynch and Dahl have extended this phenomenological approach, fitting Gaussian distributions to a variable fraction of the Molière distribution for arbitrary scatterers [25], and achieve accuracies of 2% or better.

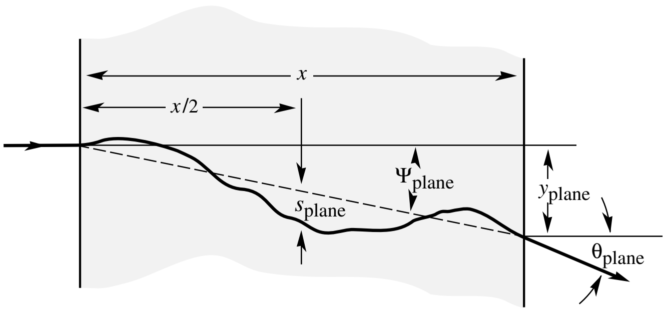

Figure 10.5: Quantities used to describe multiple Coulomb scattering. The particle is incident in the plane of the figure.

The nonprojected (space) and projected (plane) angular distributions are given approximately by [23]

$$\frac{1}{2\pi\,\theta_0^2}\exp\left(-\frac{\theta_{\rm space}^2}{2\theta_0^2}\right)d\Omega , \qquad (10.9)$$

$$\frac{1}{\sqrt{2\pi}\,\theta_0}\exp\left(-\frac{\theta_{\rm plane}^2}{2\theta_0^2}\right)d\theta_{\rm plane} , \qquad (10.10)$$

where θ is the deflection angle. In this approximation, $\theta_{\rm space}^2 \approx (\theta_{{\rm plane},x}^2 + \theta_{{\rm plane},y}^2)$, where the x and y axes are orthogonal to the direction of motion, and $d\Omega \approx d\theta_{{\rm plane},x}\,d\theta_{{\rm plane},y}$. Deflections into $\theta_{{\rm plane},x}$ and $\theta_{{\rm plane},y}$ are independent and identically distributed.